

Published in final edited form as:

*Polymer (Guildf)*. 2008 December 8; 49(26): 5692–5699. doi:10.1016/j.polymer.2008.10.021.

## Photo-Crosslinked Poly( $\epsilon$ -caprolactone fumarate) Networks: Roles of Crystallinity and Crosslinking Density in Determining Mechanical Properties

Shanfeng Wang<sup>a</sup>, Michael J. Yaszemski<sup>b,c</sup>, James A. Gruetzmacher<sup>b</sup>, and Lichun Lu<sup>b,c,\*</sup>

<sup>a</sup> Department of Materials Science and Engineering, The University of Tennessee, Knoxville, Tennessee 37996, USA

<sup>b</sup> Department of Orthopedic Surgery, Mayo Clinic College of Medicine, 200 First Street SW, Rochester, Minnesota 55905, USA

<sup>c</sup> Department of Physiology and Biomedical Engineering, Mayo Clinic College of Medicine, 200 First Street SW, Rochester, Minnesota 55905, USA

### Abstract

We present a material design strategy of combining crystallinity and crosslinking to control the mechanical properties of polymeric biomaterials. Three polycaprolactone fumarates (PCLF530, PCLF1250, and PCLF2000) synthesized from the precursor polycaprolactone (PCL) diols with nominal molecular weights of 530, 1250, and 2000 g.mol<sup>-1</sup>, respectively, were employed to fabricate polymer networks via photo-crosslinking process. Five different amounts of photo-crosslinking initiator were applied during fabrication in order to understand the role of photoinitiator in modulating the crosslinking characteristics and physical properties of PCLF networks. Thermal properties such as glass transition temperature ( $T_g$ ), melting temperature ( $T_m$ ), and degradation temperature ( $T_d$ ) of photo-crosslinked PCLFs were examined and correlated with their rheological and mechanical properties.

### Keywords

Polycaprolactone fumarate; Photo-crosslinking; Mechanical Properties

## 1. Introduction

Injectable or crosslinkable polymeric biomaterials have great advantages as they can be applied directly to fill tissue defects via in-situ hardening or fabricated into pre-formed tissue-engineering scaffolds.[1-3] Numerous novel crosslinkable copolymers have been synthesized from polycaprolactone (PCL) diol in order to further form biodegradable networks.[4-12] Without the need of introducing unsaturated segments into PCL backbone, PCL networks can be also achieved via  $\gamma$ -radiation or initiation using benzoyl peroxide at elevated temperature. [13,14] In our laboratory, several novel crosslinkable polymers and composites have been developed for hard and soft tissue engineering applications, specifically, bone and peripheral nerve regeneration.[4-6,15-19] Among these novel polymeric systems, poly(caprolactone fumarate) (PCLF) (Scheme 1) is a copolymer synthesized through the polycondensation of PCL diol and fumaryl chloride in the presence of a proton scavenger triethylamine (TEA) or

\* Corresponding author. Tel: (507) 538-4987. Fax: (507) 284-5075. lu.lichun@mayo.edu.

potassium carbonate ( $K_2CO_3$ ). [4,6] PCLF synthesized with TEA is dark in color due to the oxidization of tertiary amine while the original white color of PCL can be remained when  $K_2CO_3$  is used. [4,6] Previously, we have reported the structural analysis and physical properties of such “white” PCLFs synthesized from PCL diols with three different nominal molecular weights of 530, 1250, and 2000  $g \cdot mol^{-1}$ . [6]

Here we present the photo-crosslinking characteristics of these “white” PCLFs and their physical properties after crosslinking as a subsequent study to the previous report on uncrosslinked PCLFs [6] and also as a prelude to the serial reports on employing PCLFs in scaffold fabrication, *in vitro* cell studies, and *in vivo* biological evaluations for both bone and peripheral nerve repair. Although a few PCL networks have been reported previously, [7-14] the roles of crosslinking density and crystallinity in determining other physical properties have not yet been investigated systematically by varying both the concentration of crosslinking initiator and the molecular weight of PCL precursor. In this study, difference PCL diol molecular weight results in dramatically different thermal properties of PCLFs such as glass transition temperature ( $T_g$ ), melting temperature ( $T_m$ ), and crystallinity ( $\chi_c$ ). [6] Moreover, five different weight ratios of the photoinitiator bis(2,4,6-trimethyl benzoyl) phosphine oxide (BAPO) and PCLF have been used in the photo-crosslinking to reveal the effect of BAPO/polymer ratio on the characteristics of crosslinked PCLF networks such as gel fraction, swelling ratios in different solvents, thermal, rheological, and mechanical properties, which are all crucial in biomedical applications.

Therefore, the three PCLFs presented here are excellent model polymers for investigating the correlative effects of crystallinity and crosslinking density on the thermal, rheological, and mechanical properties of crosslinked PCLF networks. Besides supplying extensive characterizations, fabrication parameters, and properties of these novel polymeric biomaterials for tissue-engineering applications, we testify the material design strategy of combining the chemical network resulting from photo-crosslinking with the physical network formed by PCL crystallites. The controllability of mechanical properties using this design strategy suggests a good method to achieve polymeric substrates and scaffolds for regulating cell responses and tissue ingrowth. [16,20]

## 2. Materials and methods

### 2.1. Materials

All chemicals used in this study, including  $\alpha,\omega$ -telechelic PCL diols for synthesizing PCLF, were purchased from Sigma-Aldrich Co (Milwaukee, WI), unless noted otherwise. PCLF samples were synthesized using PCL diols with nominal number-average molecular weight ( $M_n$ ) of 530, 1250, and 2000  $g \cdot mol^{-1}$ . [6] Therefore, the obtained PCLFs are named as PCLF530, PCLF1250, and PCLF2000, having weight-average molecular weight ( $M_w$ ) of 6050, 15800, and 12900, and  $M_n$  of 3520, 9000, and 7300, respectively. In polycondensation, distilled fumaryl chloride, dried PCL diol, and dried  $K_2CO_3$  were measured out in a molar ratio of 0.95:1:1.2. PCL diol was dissolved in methylene chloride ( $CH_2Cl_2$ ) along with the ground  $K_2CO_3$ . The mixture was stirred to form slurry and fumaryl chloride dissolved in  $CH_2Cl_2$  was added dropwise to the slurry. The reaction mixture was maintained at 50 °C under reflux for 12 hr. The salts were completely removed from the mixture using a centrifuge. The supernatant was precipitated in ether and the wax-like product yielded after rotary evaporation and further drying in a vacuum oven.

### 2.2. Photo-crosslinking of PCLF

Photo-crosslinking was initiated with ultraviolet (UV) light ( $\lambda=315-380$  nm) in the presence of a photoinitiator BAPO (IRGACURE 819™, Ciba Specialty Chemicals, Tarrytown, NY). In

order to investigate the effect of initiator concentration on the crosslinking characteristics, five different amounts (75, 100, 125, 150, and 175  $\mu\text{L}$ ) of BAPO/ $\text{CH}_2\text{Cl}_2$  (300 mg/1.5 mL) solution were used for pre-dissolved PCLF/ $\text{CH}_2\text{Cl}_2$  solution (1.5 g/500  $\mu\text{L}$ ). BAPO/PCLF weight ratios were calculated to be 10, 13.3, 16.7, 20, and 23.3 mg/g, respectively.

Homogeneous PCLF/BAPO/ $\text{CH}_2\text{Cl}_2$  mixture was transferred into a mold consisting of two glass plates with a thickness of 2.1 mm and a Teflon spacer with a thickness of 0.37 mm. To allow crosslinking, the filled mold was placed under UV light with a distance of  $\sim 7$  cm from the lamp head for 30 min. Crosslinked PCLF sheets were removed from the mold after cooled down to ambient temperature. Strips and disks with different dimensions were cut from the sheets for different experimental purposes.

### 2.3. Structural and thermal characterizations

Fourier Transform Infrared (FTIR) spectra were obtained on a Nicolet 550 spectrometer using a zinc selenide ATR crystal. The resolution of the instrument was specified as  $4\text{ cm}^{-1}$  at  $1000\text{ cm}^{-1}$ . For achieving FTIR spectra, uncrosslinked PCLFs were dissolved in  $\text{CH}_2\text{Cl}_2$  and coated onto zinc selenide crystal while crosslinked PCLF sheets were pressed directly onto the crystal with a close contact. Differential Scanning Calorimetry (DSC) measurements were performed on a differential scanning calorimeter (Q1000, TA Instruments) in a nitrogen atmosphere. To keep the same thermal history, each sample was first heated from room temperature to  $100^\circ\text{C}$  and cooled to  $-90^\circ\text{C}$  at a cooling rate of  $5^\circ\text{C}/\text{min}$ . Then a subsequent heating run was performed from  $-90$  to  $100^\circ\text{C}$  at a heating rate of  $10^\circ\text{C}/\text{min}$ . Thermogravimetric analysis (TGA) was done in flowing nitrogen at a heating rate of  $20^\circ\text{C}/\text{min}$  using a thermal analyst (Q500, TA Instruments).

In Wide-angle X-ray Diffraction (WAXD) measurements, the waxy samples of PCL diols and PCLFs were mounted on the top of a brass pin and run in reflection mode while crosslinked PCLF disks were suspended and run in transmission mode. A Bruker AXS micro-diffractometer with copper radiation, an incident beam monochromator, and a GADDS multi-wire area detector was used for the wide angle tests. Two frames were collected, one at the Bragg angle  $2\theta=20^\circ$  and one at  $50^\circ$  to cover a range of  $5^\circ$  to  $65^\circ$  for  $2\theta$ . Each frame was collected for 5 min. The data was then integrated and plotted as intensity vs.  $2\theta$ . Peaks were identified using Material Data Incorporated's JADE 7.0 software and degree of crystallinity was determined using JADE's profile fitting program.

### 2.4. Gel fraction and swelling ratio measurements

Two crosslinked PCLF disks ( $5\text{ mm} \times 0.34\text{ mm}$ , diameter  $\times$  thickness) for each solvent were immersed in excess  $\text{CH}_2\text{Cl}_2$ , ethanol, and water. After two days, the disks were taken out and weighed after blotted quickly in order to remove the attached solvent on the surfaces. The solvent in the cubes was subsequently evacuated and the dry cubes were weighed. Based on the measured weights of the original ( $W_0$ ), dry ( $W_d$ ,  $\text{CH}_2\text{Cl}_2$  was the solvent for determining gel fractions), and fully swollen ( $W_s$ ) PCLF disks, their swelling ratios and gel fractions were calculated using the equations of  $(W_s - W_d)/W_d \times 100\%$  and  $W_d/W_0 \times 100\%$ , respectively.

### 2.5. Rheological and mechanical measurements

Linear viscoelastic properties of crosslinked PCLFs, including storage and loss moduli  $G'$  and  $G''$  as well as the viscosity  $\eta$  as functions of frequency, were measured using a dynamic mechanical spectrometer (AR2000 rheometer, TA Instruments) in the frequency ( $\omega$ ) range of 0.5-100 rad/s at 20, 37, and  $60^\circ\text{C}$ , sequentially. The rheological measurements were performed with a small strain ( $\gamma=0.01$ ) using an 8 mm diameter parallel plate flow cell and a gap of  $\sim 0.5$  mm, depending on the thickness of polymer disk.

Mechanical measurements were performed at room temperature. Tensile properties of photo-crosslinked polymer specimens were implemented by a dynamic mechanical analyzer (DMA 2980, TA instruments). In tensile measurements, polymer strips ( $\sim 30$  mm  $\times$   $\sim 2$  mm  $\times$   $\sim 0.4$  mm, length  $\times$  width  $\times$  thickness) were pulled at a rate of  $0.5$  N.min $^{-1}$  up to a maximum static force of  $18$  N. Five specimens were measured and averaged for each crosslinked PCLF. Pull-out tests were performed on a laboratory-developed mechanical analyzer for polymer disks ( $5$  mm  $\times$   $0.35$  mm, diameter  $\times$  thickness) with a loop formed using microsurgical Nylon suture (10-0 Ethilon, Ethicon Co., Somerville, NJ).[16] Three specimens for each sample were measured at a pull-out rate of  $0.1$  mm.s $^{-1}$ .

### 3. Results and Discussion

#### 3.1. Structural characterization

As depicted in Scheme 1, the flexibility of PCL renders PCLF self-crosslinkable in the absence of any other crosslinkers and crystallization will occur when the temperature is lower than its  $T_m$ . Based on the  $M_w$  of the PCLFs and their precursor PCL diols, the average numbers of PCL block ( $n$ ) can be roughly estimated to be 5, 5, and 3, respectively.[6] The number  $n$  indicates how efficiently the crosslinking could occur. FTIR spectra for uncrosslinked and crosslinked PCLFs are shown in Fig. 1. As discussed earlier,[6] absorption peaks for hydroxyl end groups (-OH) of PCL diols at around  $3200$  cm $^{-1}$  were reduced and -CH=CH- peaks at around  $1650$  cm $^{-1}$  show up in the spectra of PCLFs after the fumarate group was introduced to PCL backbone. After crosslinking, the absorption peak for -CH=CH- disappears for all the PCLFs, indicating complete consumption of unsaturated double bonds in crosslinking. It should be noted that FTIR spectra were obtained using different methods for uncrosslinked and crosslinked PCLF samples. Therefore, the intensities at absorption peaks might not be comparable quantitatively between uncrosslinked and crosslinked samples.

#### 3.2. Gel fraction and swelling ratios

Before crosslinking,  $T_g$  is around  $-60$  °C and  $T_m$  is  $29.2$ ,  $43.9$ , and  $45.7$  °C for PCLF530, 1250, and 2000, respectively.[6] As a result, PCLFs are wax- or paste-like and lack sufficient mechanical properties for biomedical applications at room temperature or body temperature. All PCLFs have been proven to be crosslinkable without the need of additional crosslinkers. As revealed in our earlier report,[6] crosslinking can be induced thermally with benzoyl peroxide and *N*-dimethyl toluidine as initiator and accelerator, respectively. Compared to thermal crosslinking, photo-crosslinking applied in the present study is faster and the crosslinked samples are not tacky.[1-3,7,16] Thus the gel fraction and physical properties of the crosslinked samples from two different crosslinking procedures can differ dramatically.

Because the composition of crosslinkable fumarate segment is lower in the PCLF synthesized from a longer PCL precursor,[6] the gel fraction of crosslinked PCLF shown in Fig. 2a decreases from PCLF530 to PCLF1250 and then PCLF2000 if the same BAPO/polymer ratio was applied. For the same PCLF, the gel fraction increases with the BAPO/polymer ratio. The gel fraction of crosslinked PCLF530 is almost identical (77-78%) to that of PCLF530 synthesized using triethylamine as the proton scavenger and crosslinked at the same BAPO/polymer ratio of  $10$  mg/g.[16] The distance between two neighboring crosslinks in PCL networks is determined by the PCL precursor's molecular weight and also the BAPO/polymer ratio. Consequently, the swelling ratio of crosslinked PCLF in CH $_2$ Cl $_2$  (Fig. 2b) increases progressively from the range of  $1.6$ - $4.0$  for crosslinked PCLF530 to  $10.9$ - $16.8$  for crosslinked PCLF2000. Meanwhile, it decreases with increasing BAPO/polymer ratio for a certain PCLF. Compared with other crosslinked polymeric systems [21], the high swelling ratios in crosslinked PCLF2000 make it potentially useful as an excellent organic solvent sorbent. All

crosslinked PCLFs do not swell in water but swell slightly in ethanol with swelling ratios ranging from 5% to 27%.

### 3.3. Thermal properties and crystalline structure

Fig. 3a shows DSC curves of crosslinked PCLFs at the BAPO/polymer ratio of 10 mg/g in both heating and cooling runs, indicated by the direction of arrow. As reported earlier,[6] PCLFs are all semi-crystalline with molecular-weight-dependent  $T_m$  and crystallinity  $\chi_c$  varying from 27.5 °C and 37.4% for PCLF530 to 43.9 °C and 47.2% for PCLF1250, then to 45.7 °C and 50.6% for PCLF2000. DSC curves in Fig. 3a show that crosslinked PCLF530 is amorphous in both heating and cooling runs because the crosslinks suppress the crystallization completely. In contrast, crosslinked PCLF1250 and 2000 are still semi-crystalline with lower crystallinities and  $T_m$  compared to their uncrosslinked counterparts. As listed in Table 1, at the BAPO/polymer ratio of 10 mg/g, the peak temperatures in the heating and cooling runs of crosslinked PCLF1250 and PCLF2000 are 31.6 and -2.6 °C, and 42 and 16.8 °C, respectively. The lower crystallization temperatures ( $T_c$ ) measured in the cooling runs indicate that supercooling is necessary for crystallization.

When the BAPO/polymer ratio increases, all the thermal properties for crosslinked PCLFs change significantly. The trend can be seen in Table 1 and also demonstrated in Fig. 3b using crosslinked PCLF1250 as a representative example because it has the most dramatic change. In PCLF networks, both crosslinks and crystallites play important roles in influencing their thermal and mechanical properties. Moreover, crystallites can be prohibited by crosslinks as found in many polymeric systems.[23] For example, imperfect crystals with a low  $T_m$  and a low  $\chi_c$  were reported previously in the crystallization of  $\epsilon$ -caprolactone blocks within a crosslinked microdomain structure of poly( $\epsilon$ -caprolactone)-block-polybutadiene.[24,25] Crosslinked PCLF530 samples at different BAPO/polymer ratios are all amorphous, indicating only crosslinks exist. While crosslinked PCLF2000 samples are all semi-crystalline with such high crystallinities and  $T_m$  that crosslinks can only suppress crystallization slightly. It can be observed in Table 1 that both  $T_m$  and  $\Delta H_m$  only decrease weakly from 42 °C and 48.4 J.g<sup>-1</sup> for crosslinked PCLF2000 at the BAPO/polymer ratio of 10 mg/g to 39.4 °C and 36.6 J.g<sup>-1</sup> at 20 mg/g. Consequently,  $T_g$  increases in crosslinked PCLF530 and PCLF2000 with increasing the BAPO/polymer ratio because a higher density of crosslinks limits the motion of molecular segments more efficiently. Unlike crosslinked PCLF530 and 2000, crosslinked PCLF1250 involves a higher density of crosslinks and reduced crystallinity when a higher BAPO/polymer ratio was applied in its crosslinking. As shown in Fig. 3b and Table 1,  $T_c$  in the cooling run decreases significantly with reducing  $\Delta H_m$ . Due to the significant decrease in  $T_m$  and  $\Delta H_m$ ,  $T_g$  decreases slightly instead for crosslinked PCLF1250 when the BAPO/polymer ratio increases, which is on the contrary to the trend observed in the other two crosslinked PCLFs.

The crystalline structures of PCL diols, uncrosslinked PCLFs, and crosslinked PCLFs are demonstrated in WAXD patterns in Fig. 4. PCLF samples show the same diffraction peaks at  $2\theta=20.2$ , 21.4, 22.0, 23.7, and 30.0° as their precursor PCL diols, corresponding to  $d$ -spacings of 0.440, 0.415, 0.403, 0.375, and 0.295 nm.[26,27] After crosslinking at the BAPO/polymer ratio of 10 mg/g, the diffraction peak at  $2\theta=22.0^\circ$  is no longer prominent for all three crosslinked PCLFs and there is only a broad diffraction peak at  $2\theta=20.2^\circ$  ( $d=0.440$  nm) for crosslinked PCLF530, confirming its amorphous characteristics. From the diffraction peaks in Fig. 4, crystallinities for both uncrosslinked and crosslinked PCLFs can be calculated. PCLF530, 1250, and 2000 have crystallinities of 20%, 48%, and 54%, which decrease to 0%, 37%, and 53% after crosslinking, respectively. It should be noted that the crystallinity obtained from DSC (Table 1) is lower because of different thermal history of the measured samples.

Thermogravimetric analysis (TGA) has been performed to determine the thermal stability of both uncrosslinked and crosslinked PCLFs. As demonstrated in Fig. 5, all samples show one

single degradation step. The enlarged area in the inset of Fig. 5 shows the onset thermal degradation temperature ( $T_d$ ) decreases for all three PCLFs after crosslinking, in a clear contrast with both the much higher  $T_d$  ( $>600$  °C) values and the opposite trend reported earlier on another PCL network.[11]  $T_d$  for crosslinked PCLF530, 1250, and 2000 in this study is 368, 382, and 385 °C, respectively, while the values are 390, 399, and 399 °C for their uncrosslinked counterparts. Varying the BAPO/polymer ratio in crosslinking does not affect  $T_d$  noticeably.

### 3.4. Rheological properties

Fig. 6 shows dynamic frequency sweep results of crosslinked PCLFs at 20, 37, and 60 °C, revealing the rheological properties at three different conditions: room temperature, body temperature, and amorphous state in which all the crystallites have been melted. The BAPO/polymer ratio is 10 mg/g for these crosslinked PCLFs. All the curves show rubbery region with  $G'$  always larger than  $G''$  and no frequency dependence for  $G'$  in the range of 0.5-100 rad/s. Meanwhile, shear thinning behavior can be observed for viscosity.

Because crosslinked PCLF530 is amorphous as indicated in the DSC curve in Fig. 2a and WAXD pattern in Fig. 4, the curves for storage modulus  $G'$ , loss modulus  $G''$ , and viscosity  $\eta$  in Fig. 6a do not vary with the measurement temperature. In contrast, both crosslinked PCLF1250 and 2000 show clear variance with measurement temperature in Figs. 6b and 6c, respectively. Because its  $T_m$  is 42.0 °C (Table 1),  $G'$  and  $\eta$  for crosslinked PCLF2000 remain the same values at 20 and 37 °C. When the measurement temperature is 60 °C, a dramatic decrease occurs in all the parameters of  $G'$ ,  $G''$ , and  $\eta$ , as indicated in Fig. 6c. Crosslinked PCLF1250 in Fig. 6b shows a continuous decrease in  $G'$ ,  $G''$ , and  $\eta$  with increasing measurement temperature. As mentioned in thermal properties, both crosslinks and crystallites play important roles in determining rheological and mechanical properties. Thus the magnitude of  $G'$  (12 MPa) for crosslinked PCLF1250 is over ten times higher than that (1.1 MPa) for crosslinked PCLF530 at 20 °C because the crystallites enhance the PCLF1250 network significantly as physical fillers or associations. Because crosslinked PCLF1250's  $T_m$  is 31.6 °C, crystalline domains start to melt partially at the measurement temperature of 37 °C and will diminish at 60 °C. Correspondingly, the magnitude of  $G'$  drops to 4.8 MPa at 37 °C and then to 0.14 MPa at 60 °C, as shown in Fig. 6b.

When the PCLF networks are amorphous at 60 °C, there is no role of crystallites and only chemical crosslinks exist. It can be observed that the magnitude of  $G'$  (or plateau modulus) decreases from 1.1 MPa for crosslinked PCLF530 to 0.14 MPa for crosslinked PCLF1250, and then to 0.064 MPa for crosslinked PCLF2000. Because the plateau modulus in a polymer network is inversely proportional to the molecular weight between two neighboring crosslinks, [16,28] the decrease in plateau modulus can be largely attributed to the increase in the molecular weight of precursor PCL diol from 530 to 1250, and 2000 g/mol. It should be noted that the molecular weights determined by GPC are different from their nominal molecular weights as discussed in our earlier report and PCLF530 has a higher density of crosslinkable segment that results in an even denser network.[6]

### 3.5. Mechanical properties

Mechanical properties of crosslinked PCLF from tensile and pull-out measurements at room temperature are shown in Fig. 7. For tensile and pull-out tests, five BAPO/polymer ratios were used to investigate the effect of photoinitiator concentration on the mechanical properties of crosslinked PCLFs. As discussed earlier, different BAPO/polymer ratio results in different crosslinking density that consequently influences the gel fraction,  $T_m$ , and crystallinity of the PCLF network. If the measurement is performed at temperature lower than its  $T_m$ , crystallites can be considered as physical fillers to enhance mechanical properties as indicated in plateau modulus in oscillatory shear experiments in Fig. 6. Because crosslinked PCLF530 is

amorphous at all BAPO/polymer ratios, its tensile modulus and stress at break are as low as  $0.87\pm 0.07$  and  $0.48\pm 0.40$  MPa, shown in Figs. 7a and 7b, respectively. With increasing BAPO/polymer ratio, these two properties increase while elongation at break decreases because of a higher crosslinking density. For crosslinked PCLF2000 with the highest crystallinity and  $T_m$  among these three crosslinked PCLFs, the BAPO/polymer ratio only influence the crystallinity weakly as demonstrated in Table 1. Therefore, PCLF2000 networks with the enhancement of crystallites possess the highest tensile modulus and stress at break as well as pull-out force.

Because the  $T_m$  for crosslinked PCLF1250 is close to room temperature, there is a strong BAPO/polymer ratio dependence for all the mechanical properties as shown in Figs. 7a-d. When the BAPO/polymer ratio exceeds 16.7 mg/g, PCLF1250 networks have low tensile moduli and stresses at break that are comparable to the amorphous crosslinked PCLF530 without being enhanced by crystallites. Crosslinked PCLF2000 has a low gel fraction of 52% at the BAPO/polymer ratio of 10 mg/g. Consequently, it is very brittle with a high tensile modulus of  $138\pm 17$  MPa and a low elongation at break of  $16.6\pm 2.3\%$ . After the PCLF2000 network has a higher gel fraction ( $>60\%$ ) at a higher BAPO/polymer ratio, it becomes tougher as indicated by a higher elongation at break between  $79\pm 30\%$  and  $117\pm 30\%$ .

Pull-out force is an important parameter to judge if a material can hold suture to ensure the connection between the polymeric nerve conduits and the proximal and distal nerve ends during the implantation.[16] Consistent with their tensile modulus and tensile stress at break, crosslinked PCLFs demonstrate a similar trend in the effect of BAPO/polymer ratio on pull-out force. The pull-out force increases weakly from  $0.053\pm 0.002$  to  $0.064\pm 0.0003$  N for crosslinked PCLF530 while it decreases from  $0.24\pm 0.03$  to  $0.10\pm 0.006$  N for crosslinked PCLF1250 as the BAPO/polymer ratio increases from 10 to 23.3 mg/g. Due to higher crystallinities, PCLF2000 networks have much higher pull-out forces of around 0.43 N, which suggests that crosslinked PCLF2000 is more suitable for being used as a nerve conduit material than the other two PCLFs.

Our laboratory recently has focused on the injectable polymeric systems with controllable mechanical properties for investigating the role of mechanical factor in regulating cell responses and tissue ingrowth.[16] The present study supplied a comprehensive understanding on how to achieve different mechanical properties by using different PCLF networks with controlled crystallinity and crosslinking density. The other polymeric systems include a series of copolymers consisting of polypropylene fumarate (PPF) and PCL, PPF/PCLF blends,[16] and PPF [19] or PCLF composites with hydroxyapatite nano-particles. A subsequent report will be elaborated on the controllability of cell responses on these different photo-crosslinked PCLF networks and the criteria of selecting biomaterials with appropriate mechanical properties for guided peripheral nerve regeneration.

## 4. Conclusions

Three polycaprolactone fumarates (PCLFs) with different molecular weights of the precursor polycaprolactone (PCL) diol have been photo-crosslinked in the presence of a photoinitiator, bis(2,4,6-trimethyl benzoyl) phosphine oxide (BAPO). Five different BAPO/polymer ratios have been applied in the crosslinking and the role of BAPO/polymer ratio in influencing the physical properties of crosslinked PCLFs has been studied extensively. It is verified that the photoinitiator can be used to modulate the physical properties of crystalline polymer networks via the correlative effects of crosslinking density and crystallinity. Because different PCLFs have different crystallinity and melting temperature, the effect of BAPO/polymer ratio is strikingly distinct for each of them. Crosslinked PCLF530, which was synthesized from a PCL diol with a nominal molecular weight of  $530 \text{ g}\cdot\text{mol}^{-1}$ , is amorphous at all the studied BAPO/polymer ratios because the crosslinks suppress crystallization completely. In contrast,

crosslinked PCLF2000 from a PCL diol with a nominal molecular weight of 2000 g.mol<sup>-1</sup> has the highest T<sub>m</sub> and crystallinity among these three crosslinked PCLFs. By combining chemical crosslinks and physical associations between crystalline domains, crosslinked PCLF2000 has the highest rheological and mechanical properties at body temperature.

## Acknowledgments

This work was performed at Mayo Clinic with the supports from the Mayo Foundation and NIH (R01 AR45871 and R01 EB003060). The authors thank Mark E. Zobitz for technical assistance in pull-out tests. WAXD measurements were carried out by Ryan Wold and Linda Sauer in the Institute of Technology Characterization Facility, University of Minnesota, which receives partial support from NSF through the NNIN program.

## References

1. Anseth KS, Shastri VR, Langer R. Photopolymerizable degradable polyanhydrides with osteocompatibility. *Nature Biotech* 1999;17(2):156–9.
2. Fisher JP, Dean D, Engel PS, Mikos AG. Photoinitiated polymerization of biomaterials. *Annu Rev Mater Res* 2001;31:171–181.
3. Ifkovits JL, Burdick JA. Photopolymerizable and degradable biomaterials for tissue engineering applications. *Tissue Eng* 2007;13(10):2369–95. [PubMed: 17658993]
4. Jabbari E, Wang SF, Lu LC, Gruetzmacher JA, Ameenuddin S, Hefferan TE, Currier BL, Windebank AJ, Yaszemski MJ. Synthesis, material properties and biocompatibility of a novel self-crosslinkable poly(caprolactone fumarate) as an injectable tissue engineering scaffold. *Biomacromolecules* 2005;6(5):2503–11. [PubMed: 16153086]
5. Wang S, Lu L, Gruetzmacher JA, Currier BL, Yaszemski MJ. A biodegradable and cross-linkable multiblock copolymer consisting of poly(propylene fumarate) and poly( $\epsilon$ -caprolactone): Synthesis, characterization, and physical properties. *Macromolecules* 2005;38(17):7358–70.
6. Wang S, Lu L, Gruetzmacher JA, Currier BL, Yaszemski MJ. Synthesis and characterizations of biodegradable and crosslinkable poly( $\epsilon$ -caprolactone fumarate), poly(ethylene glycol fumarate), and their amphiphilic copolymer. *Biomaterials* 2006;27(6):832–41. [PubMed: 16102819]
7. Turunen MPK, Korhonen H, Tuominen J, Seppälä JV. Synthesis, characterization and crosslinking of functional star-shaped poly( $\epsilon$ -caprolactone). *Polym Int* 2001;51(1):92–100.
8. Lendlein A, Schmidt AM, Langer R. AB-polymer networks based on oligo( $\epsilon$ -caprolactone) segments showing shape-memory properties. *Proc Natl Acad Sci USA* 2001;98:842–7. [PubMed: 11158558]
9. Nagata M, Kanechika M, Sakai W, Tsutsumi N. Biodegradable network elastomeric polyesters from multifunctional aromatic carboxylic acids and poly( $\epsilon$ -caprolactone) diols. *J Polym Sci Polym Chem* 2002;40(24):4523.
10. Ramos, M.; Huang, SJ. Functional Hydrophilic-hydrophobic hydrogels derived from condensation of polycaprolactone diol and poly(ethylene glycol) with itaconic anhydride. In: Carraher, CE., Jr; Swift, GG., editors. *Functional Condensation Polymers*. New York: Kluwer Academic/Plenum Publishers; 2002. p. 185-98.
11. Kweon HY, Yoo MK, Park IK, Kim TH, Lee HC, Lee HS, Oh JS, Akaike T, Cho CS. A novel degradable polycaprolactone networks for tissue engineering. *Biomaterials* 2003;24:801–8. [PubMed: 12485798]
12. Nagata M, Kato K, Sakai W, Tsutsumi N. Biodegradable network elastomeric polyesters from multifunctional aliphatic carboxylic acids and poly ( $\epsilon$ -caprolactone) diols. *Macromol Biosci* 2006;6(5):333–9. [PubMed: 16676379]
13. Han C, Ran X, Su X, Zhang K, Liu N, Dong L. Effect of peroxide crosslinking on thermal and mechanical properties of poly( $\epsilon$ -caprolactone). *Polym Inter* 2007;56:593–600.
14. Zhu G, Xu Q, Qin R, Yan H, Liang G. Effect of  $\gamma$ -radiation on crystallization of polycaprolactone. *Radiat Phys Chem* 2005;74:42–50.
15. Wang S, Lu L, Yaszemski MJ. Bone-tissue-engineering material poly(propylene fumarate): Correlation between molecular weight, chain dimensions, and physical properties. *Biomacromolecules* 2006;7(6):1976–82. [PubMed: 16768422]



16. Wang S, Kempen DH, Simha NK, Lewis JL, Windebank AJ, Yaszemski MJ, Lu L. Photo-cross-linked hybrid polymer networks consisting of poly(propylene fumarate) and poly(caprolactone fumarate): controlled physical properties and regulated bone and nerve cell responses. *Biomacromolecules* 2008;9(4):1229–41. [PubMed: 18307311]
17. Lee KW, Wang S, Lu L, Jabbari E, Currier BL, Yaszemski MJ. Fabrication and characterization of poly(propylene fumarate) scaffolds with controlled pore structures using three-dimensional printing and injection molding. *Tissue Eng* 2006;12(10):2801–11. [PubMed: 17518649]
18. Lee KW, Wang S, Fox B, Ritman EL, Yaszemski MJ, Lu L. Poly(propylene fumarate) bone tissue engineering scaffold fabrication using stereolithography: Effects of resin formulations and laser parameters. *Biomacromolecules* 2007;8(4):1077–84. [PubMed: 17326677]
19. Lee KW, Wang S, Yaszemski MJ, Lu L. Physical properties and cellular responses to crosslinkable poly(propylene fumarate)/hydroxyapatite nanocomposites. *Biomaterials* 2008;29(19):2839–48. [PubMed: 18403013]
20. Discher DE, Janmey P, Wang YL. Tissue cells feel and respond to the stiffness of their substrate. *Science* 2005;310:1139–43. [PubMed: 16293750]
21. Sonmez HB, Wudl F. Crosslinked poly(orthocarbonate)s as organic solvent sorbents. *Macromolecules* 2005;38(5):1623–6.
22. Brandrup, J.; Immergut, EH., editors. *Polymer handbook*. 3rd. New York: Wiley; 1989.
23. Mandelkern, L. *Crystallization of Polymers*. 2nd. Vol. 1. New York: McGraw-Hill; 2001. Chapter 7
24. Nojima S, Tanaka H, Rohadi A, Sasaki S. The effect of glass transition temperature on the crystallization of  $\epsilon$ -caprolactone-styrene diblock copolymers. *Polymer* 1997;39(8-9):1727–34.
25. Nojima S, Hashizume K, Rohadi A, Sasaki S. Crystallization of  $\epsilon$ -caprolactone blocks within a crosslinked microdomain structure of poly( $\epsilon$ -caprolactone)-block-polybutadiene. *Polymer* 1997;38(11):2711–8.
26. Bittiger H, Marchess RH, Niegisch WD. Crystal structure of poly- $\epsilon$ -caprolactone. *Acta Cryst* 1970;B26:1923–7.
27. Lovinger AJ, Han BJ, Padden FJ Jr, Mirau PA. Morphology and properties of polycaprolactone-poly(dimethyl siloxane)-polycaprolactone triblock copolymers. *J Polym Sci Part B Polym Phys* 1993;31(2):115–23.
28. Sperling, LH. *Introduction to Physical Polymer Science*. 3rd. Wiley; New York: 2001.

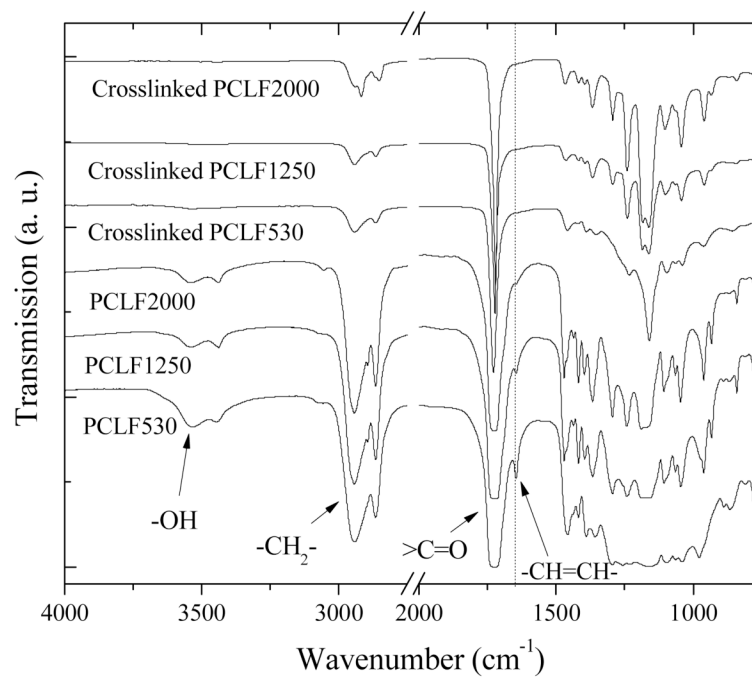


**Fig. 1.** FTIR spectra of uncrosslinked and crosslinked PCLFs.

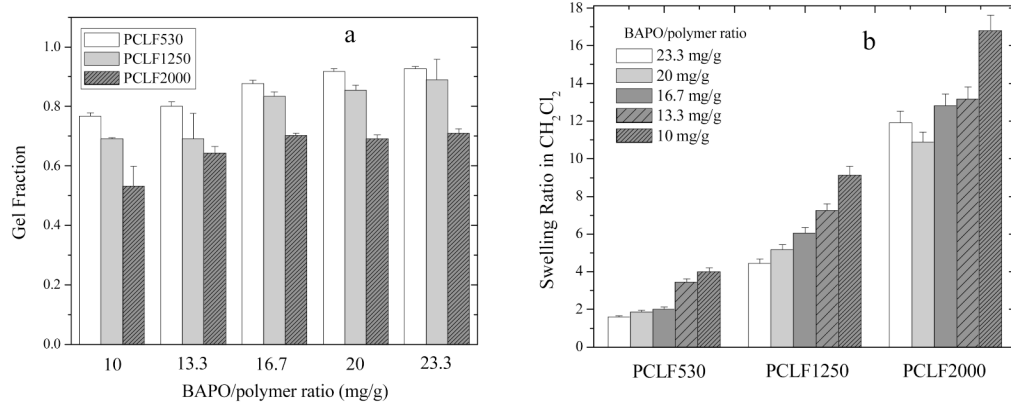


**Fig. 2.** (a) Gel fractions of crosslinked PCLFs after being soaked in CH<sub>2</sub>Cl<sub>2</sub>, (b) swelling ratios of crosslinked PCLFs in CH<sub>2</sub>Cl<sub>2</sub>.

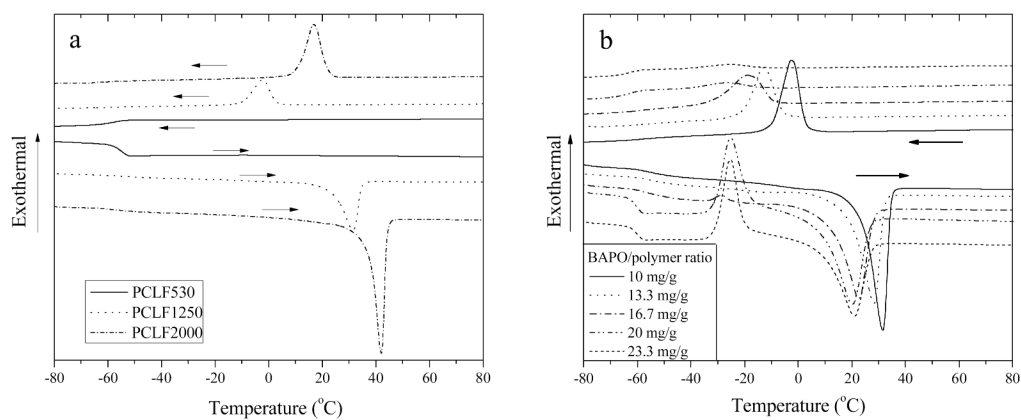


**Fig. 3.** DSC curves of (a) crosslinked PCLFs at BAPO/polymer ratio of 10 mg/g and (b) crosslinked PCLF1250 at different crosslinking conditions recorded in both cooling and heating runs with arrows to indicate the temperature change direction.

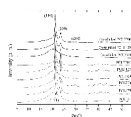


**Fig. 4.** WAXD patterns of PCL diols, PCLFs, and crosslinked PCLFs at BAPO/polymer ratio of 10 mg/g.

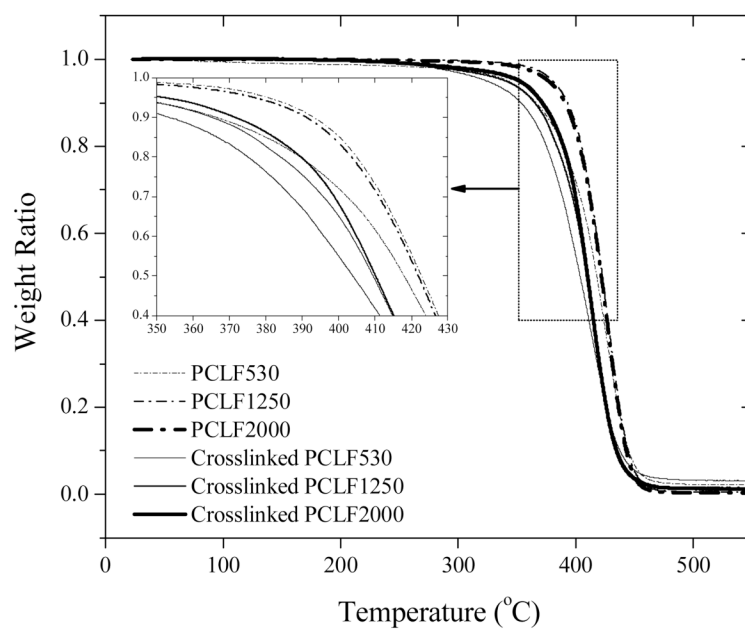


**Fig. 5.** TGA thermograms of uncrosslinked and crosslinked PCLFs at BAPO/polymer ratio of 10 mg/g. Inset: enlarged thermal degradation curves for the dotted area.

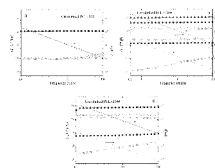


**Fig. 6.** Storage modulus  $G'$  (solid symbols), loss modulus  $G''$  (open symbols), and viscosity  $\eta$  (lines) vs frequency for crosslinked PCLFs (a: PCLF530, b: PCLF1250, c: PCLF2000) at the BAPO/polymer ratio of 10 mg/g and measurement temperatures of 20 °C (triangles and solid lines), 37 °C (circles and dashed lines), and 60 °C (squares and dotted lines).

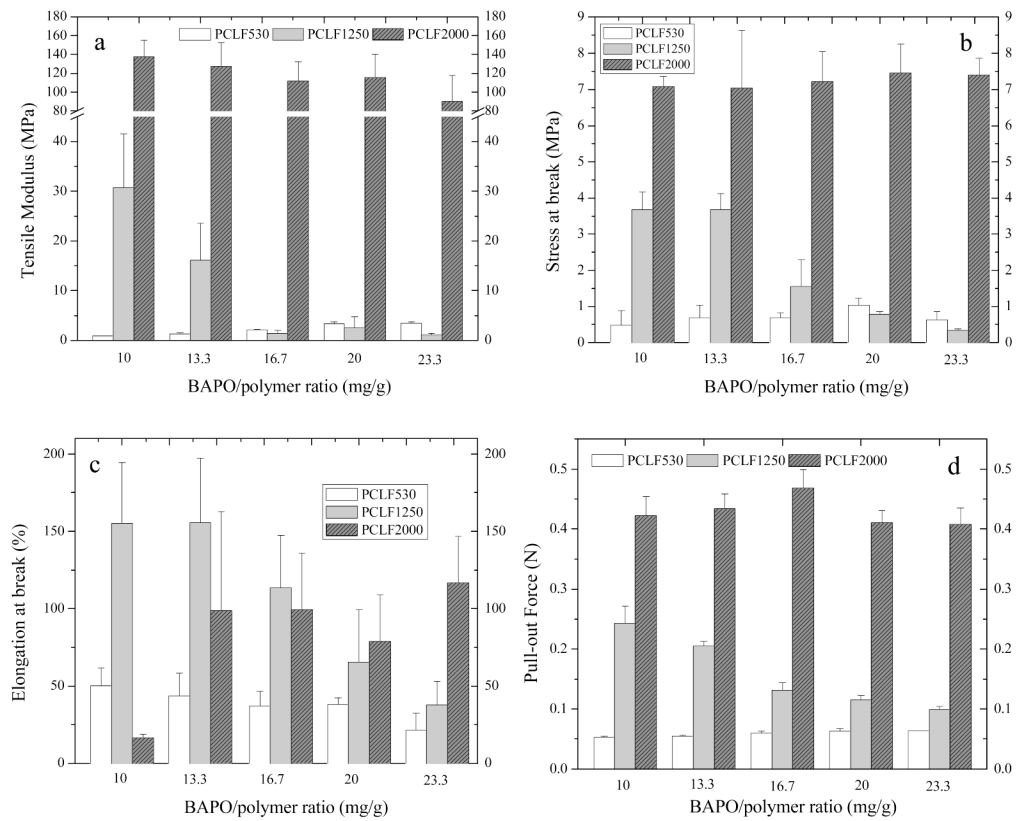
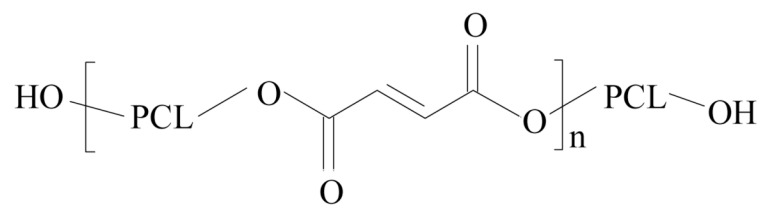


**Fig. 7.** Mechanical characteristics such as (a) tensile modulus, (b) tensile stress at break, (c) tensile strain at break, and (d) pull-out force of crosslinked PCLF specimens at different crosslinking conditions.





**Scheme 1.**  
Chemical structure of PCLF.

Table 1

Thermal properties of crosslinked PCLFs at different BAPO/polymer ratios

BAPO/polymer (mg/g)	T <sub>g</sub> (°C)		T <sub>m</sub> or T <sub>c</sub> (°C) <sup>a</sup>		ΔH <sub>m</sub> (J.g <sup>-1</sup> ) <sup>a</sup>		χ <sub>c</sub> <sup>b</sup>		
	PCLF530	PCLF1250	PCLF2000	PCLF1250	PCLF2000	PCLF1250	PCLF2000	PCLF1250	PCLF2000
10	-54.7	-55.1	-59.0	31.6 (-2.6)	42.0 (16.8)	38.9 (39.7)	48.4 (50.7)	0.30	0.37
13.3	-54.5	-56.0	-56.5	28.2 (-13.2)	41.0 (14.3)	34.7 (32.0)	46.8 (49.0)	0.27	0.35
16.7	-52.7	-59.0	-57.7	22.6 (-19.0)	39.4 (7.7)	30.1 (25.4)	41.4 (45.7)	0.23	0.31
20	-52.2	-60.0	-57.3	20.3 (-26.5)	39.4 (10.4)	31.7 (6.0)	36.6 (40.0)	0.25	0.28
23.3	-51.8	-60.4	-56.7	21.1 (-25.7)	39.5 (12.1)	30.1 (4.4)	--	0.23	--

<sup>a</sup> T<sub>m</sub> and ΔH<sub>m</sub> out of parenthesis, and T<sub>c</sub> and ΔH<sub>m</sub> in parenthesis were determined in the heating and cooling runs of DSC, respectively.

<sup>b</sup> Crystallinity χ<sub>c</sub> was calculated using the equation of  $\chi_c = [\Delta H_m / (\phi_{PCL} \Delta H_m^0)] \times 100\%$ , where ΔH<sub>m</sub><sup>c</sup> of PCL is 135 J/g [22] and φ<sub>PCL</sub> is 95.7% and 98.1% [6] for crosslinked PCLF1250 and PCLF2000, respectively.